 doi:10.20944/preprints202010.0586.v1

Publications of the Astronomical Society of Australia

The Effects of Inertial Forces on the Dynamics of Disk Galaxies

R. Gomel[1], T. Zimmerman[2]
[1]School of Physics and Astronomy, Tel Aviv University, Ramat Aviv 69978, Israel, roygomel@post.tau.ac.il
[2]School of Physics and Astronomy, Tel Aviv University, Ramat Aviv 69978, Israel, stomerzi@gmail.com

Abstract

When dealing with galactic dynamics, or more specifically, with galactic rotation curves, one basic assumption is always taken: the frame of reference relative to which the rotational velocities are given is assumed to be inertial. In other words, fictitious forces are assumed to vanish relative to the *observational frame* of a given galaxy. It might be interesting, however, to explore the outcomes of dropping that assumption; that is, to search for signatures of non-inertial behavior in the observed data. In this work, we show that the very discrepancy in galaxy rotation curves could be attributed to non-inertial effects. We derive a model for spiral galaxies that takes into account the possible influence of fictitious forces and find that the additional terms in the new model, due to fictitious forces, closely resemble dark halo profiles. Following this result, we apply the new model to a wide sample of galaxies, spanning a large range of luminosities and radii. It turns out that the new model accurately reproduces the structures of the rotation curves and provides very good fittings to the data.

Keywords: reference systems – galaxies: kinematics and dynamics – cosmology: dark matter

1 INTRODUCTION

One of the major tools to analyze the dynamics and mass distributions of disk galaxies is a *Rotation Curve* (Sofue & Rubin, 2001). It presents the variation in the orbital velocities within a galaxy at different distances from the center. Its introduction, however, gave rise to a fundamental discrepancy: Newtonian predictions seemed to be incompatible with actual observations. According to Newtonian dynamics, the rotational velocities at the outskirts of galaxies should decrease with distance. However, actual observations did not show such a trend (Babcock, 1939; Salpeter, 1978; Rubin, Ford & Thonnard, 1980; Sancisi & van Albada, 1987). An illustration of the discrepancy is presented in Fig. 1.

Two different approaches to dealing with the discrepancy have emerged over the years. One approach poses that Newtonian models are missing additional mass (i.e. dark matter), while the second approach argues that the very application of Newton's laws is invalid in these cases (Milgrom, 1983). The vast majority of astrophysicists support the first explanation as dark matter explains much more than only rotation curves. Dark matter is a major ingredient in current cosmology, explaining the CMB (Jarosik et al., 2011), structure formation (del Popolo, 2007), the discrepancies in galaxy clusters (Massey, Kitching & Richard, 2010), merging galaxy clusters (Markevitch et al., 2004), and more.

In the field of galaxy dynamics, and specifically in disk galaxies with measured rotation curves, a basic assumption has always been made: the frame of reference, relative to which the observed rotational velocities are given, is assumed to be inertial (e.g. the black points in Fig. 1 are assumed to be given relative to an inertial frame of reference). In such frames fictitious forces do not arise, and therefore their influence should not be taken into account in the models. Indeed, the blue curve in Fig. 1 (i.e. the baryonic rotation curve) does not include any contribution of fictitious forces.

This current work explores the consequences of dropping the basic assumption. What if the observed rotational velocities (of each and every galaxy) cannot be treated as inertial? In the next section we show that when defining the local inertial frame of a given galaxy by relying on the physical constraints alone, and avoiding any cosmological interpretation, a single (hidden) degree of freedom is revealed. That is, the

Preprints (www.preprints.org) | NOT PEER-REVIEWED | Posted: 28 October 2020 doi:10.20944/preprints202010.0586.v1

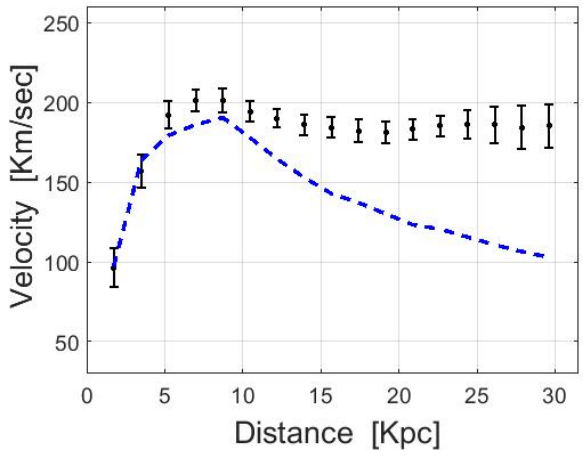

Figure 1. A measured rotation curve (black points with error-bars) and its Newtonian prediction (dashed blue line). The predicted curve is based on visible matter alone. The inconsistency with the observed data is known as *the discrepancy in galaxy rotation curves*. The data (NGC 4157) was taken from McGaugh's Data Pages (McGaugh, 2017).

observational frame (where the RC is presented) and the local inertial frame (where Newton's laws are valid) do not necessarily coincide. We also show that the recent observations of Lee et al. (2019) are consistent with such a view.

Motivated by this insight, we derive a new model for the rotational velocities. The new model includes an additional term due to the transformation of the velocities between the frames. It turns out that the contribution of the additional term to the rotational velocities is similar to the contribution of common dark halo profiles (e.g. NFW, Burkert). This surprising result might have implications other than those directly related to rotation curves. However, these implications should be discussed separately and independently.

This paper is organized as follows: Section 2 derives a new model for the rotational velocities, i.e. a model for disk galaxies that takes into account the influence of inertial forces. Section 3 demonstrates that this model is effectively similar to common dark halo profiles. Section 4 uses this model to fit a wide sample of rotation curves, and in Section 5 we conclude and discuss future directions.

2 DERIVING A NEW MODEL

One of the main results of the general theory of relativity (GR) is the insight that a gravitational field could arise not only by means of mass distributions, but also due to the state of motion of the frame itself (Einstein, 1920). That is, with respect to an "accelerating" or a "rotating" frame of reference, a gravitational field would appear. Although the weak-field approximation is used in the regime of galactic dynamics, this basic insight still holds: a gravitational field would appear if the frame is non-inertial. The *frame*, in this context, is simply the observational frame of reference, relative to which the data is presented. The *gravitational field*, in this context, is simply the field due to classical fictitious forces. If indeed such a field exists relative to the observational frame of a given galaxy, it may "play the role" of a dark halo. But first, can the observational frame be non-inertial?

Let us introduce frame K, which is assumed to be inertial, at least locally. That is, a frame of reference relative to which the behavior of bodies in a specific disk galaxy could be described by applying Newton's laws of motion. Without loss of generality, this frame can always be arranged with its $x-y$ plane aligned with the galactic plane and its origin aligned with the galactic center (see Fig. 2). The reason for this stems from the nature of the central-force problem: if Newton's laws are to be valid relative to that frame, then, assuming a central-force problem, each body would preserve its plane of motion. Therefore, the whole galactic plane would be "stationary" relative to that frame. It is now only a matter of definition to call it "the $x-y$ plane".

Next, we introduce a second system of coordinates, K', relative to which the RC data of a given disk galaxy is presented (i.e. the "observational" frame). Note that the RC data *must* be given relative to some frame of reference. In Appendix A, we show that this frame of reference can be chosen such that its $x'-y'$ plane is aligned with the galactic plane and its origin with the galactic center. We also show that K' is constrained: the line-of-sight connecting the observer and the specific galaxy must be "fixed" relative to that frame (see Fig. 2). This results directly from using line-of-sight velocities when deriving a rotation curve.

Without any further information, one has no basis to assume the coincidence of K and K'. There is a possible relative motion between the two systems: an angular velocity of one system relative to the $z-axis$ of the other. Therefore, the observational frame K' could in principle be non-inertial. Recent observations seem to support this result: Lee et al. (2019) used the line-of-sight velocity measurements of 434 disk galaxies to show that the rotational direction of a galaxy is coherent with the average motion of its neighbors. Using our notations, this means that the neighbors of a given disk galaxy were found to orbit (on average) around the origin of frame K'. The "neighbors", in this context, are galaxies located up to 15 Mpc from the given disk galaxy. Such a rotation could, in general,

Preprints (www.preprints.org) | NOT PEER-REVIEWED | Posted: 28 October 2020 doi:10.20944/preprints202010.0586.v1

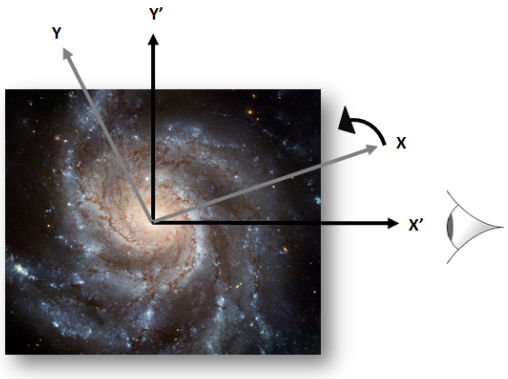

Figure 2. The measured velocities presented in RCs are valid only with respect to K', by definition. If K' is not inertial, then the relative motion between K (the inertial frame) and K' (the observational frame) includes only rotation. For the sake of simplicity, in this figure the observer is located on the galactic plane. The definitions of K and K', however, hold for any observer.

be responsible for the introduction of inertial forces in K' (Thirring, 1918; Brill & Cohen, 1966; Schmid, 2006), or, in different words, be responsible for the "dragging" of the local inertial frame K . However, let us clarify: explaining or modeling the surprising results found by Lee et al. (2019) is not included in the scope of this work. We mention their results as it seems to be consistent with the view presented in this work. In order to model the rotational velocities in K' we take a different approach.

We treat the possible angular velocity between K and K' (of a given galaxy) as a free parameter. In accordance with the previous definitions, our goal is to derive a model for the rotational velocities $v_{K'}(r)$ in K'. For this purpose, a relation between the velocities $v_{K'}(r)$ and $v_K(r)$ should be found. By using such a relation and the known model for $v_K(r)$, the velocities $v_{K'}(r)$ could be extracted. The model for $v_K(r)$, in this context, is simply the Newtonian model using a baryonic mass distribution (e.g. the blue curve in Fig. 1).

Finding such a relation is quite straightforward. However, it would be beneficial to derive it from the relation between the accelerations. Given a frame of reference K', rotating at a constant angular velocity $\boldsymbol{\omega}$ relative to an inertial frame K, the relation between the accelerations in the two frames is given by:

$$\mathbf{a_{K'}} = \mathbf{a_K} - 2\boldsymbol{\omega} \times \mathbf{v_{K'}} - \boldsymbol{\omega} \times (\boldsymbol{\omega} \times \mathbf{r_{K'}}), \qquad (1)$$

where $\mathbf{a_K}$ ($\mathbf{a_{K'}}$) is the acceleration of a body relative to K (K'), $\boldsymbol{\omega}$ is the constant angular velocity at which system K' revolves relative to system K, $\mathbf{v_{K'}}$ is the velocity of the body relative to K' and $\mathbf{r_{K'}}$ is the position of the body relative to K'. Note that the Coriolis term, $-2\boldsymbol{\omega} \times \mathbf{v_{K'}}$, and the centrifugal term, $-\boldsymbol{\omega} \times (\boldsymbol{\omega} \times \mathbf{r_{K'}})$, are present in the transformation.

In our case it would be more convenient to define a positive angular velocity in the opposite direction, as can be seen in Fig. 2. Therefore, taking $\omega \to -\omega$ and assuming that a body performs a counterclockwise uniform circular motion, leads to the following relation in the $\hat{\boldsymbol{r}}$ direction:

$$-\frac{v_{K'}^2}{r} = -\frac{v_K^2}{r} - 2\omega v_{K'} + \omega^2 r, \qquad (2)$$

where v_K ($v_{K'}$) is the magnitude of the rotational velocity relative to K (K') , ω is the constant angular velocity at which system K revolves around the $z'-axis$ of system K' and r is the radius of the circular motion.

At this stage, a useful sanity check could already be done. We recall that a dark halo produces an extra force in the inward direction. Therefore, we have to make sure that the two fictitious forces combined, could also act in the inward direction. Looking at Eq. (2), one can see that this condition is satisfied when $\omega^2 r < 2\omega v_{K'}$, or $0 < \omega < \frac{2v_{K'}}{r}$. For a given galaxy and a given observed rotation curve $v_{K'}(r)$, this inequality sets limits on ω. Within these limits, one can find an ω which produces an inward net force in K' at any radius. Whether this additional force could imitate the behavior of dark halo profiles is the subject of the following section.

Next, solving Eq. (2), we find:

$$v_{K'}(r) = v_K(r) + \omega r. \qquad (3)$$

Eq. (3) is the essence of this work. The velocities $v_{K'}(r)$ are the new model for the rotational velocities. The idea is that the expected Keplerian behavior (for the rotational velocities) could be measured only relative to K. The observational frame K', however, differs from K when $\omega \neq 0$ (see Fig. 2). In that case, the model for the rotational velocities should include an additional linear term (ωr). In the next section we show that the additional term can effectively "play the role" of a dark halo. In section 4 we show that the new model can be used to fit a large sample of rotation curves.

3 INERTIAL FORCES AS AN EFFECTIVE DARK HALO

It is well known that dark halos are used successfully to fit all sorts of RCs (Carignan, 1985; Corbelli & Salucci, 2000; de Blok et al., 2008). It would be beneficial, therefore, to explore whether our model can imitate the behavior of some common dark-halo profiles. In this section, we wish to derive an effective dark component, with a

Preprints (www.preprints.org) | NOT PEER-REVIEWED | Posted: 28 October 2020 doi:10.20944/preprints202010.0586.v1

velocity distribution $V_{dark}(r)$, which would be equivalent to the new model. To that end, the following condition must be satisfied:

$$\sqrt{V^2_{baryonic}(r) + V^2_{dark}(r)} = V_{inertial}(r) + \omega r. \quad (4)$$

The left-hand side is simply the model for the rotational velocities in the presence of a dark halo. The right-hand side is our new model for the rotational velocities. Using a dark component with a distribution $V_{dark}(r)$ which satisfies the above equation, is effectively the same as using the new model.

Before proceeding, note that the terms $V_{baryonic}(r)$ and $V_{inertial}(r)$ refer exactly to the same thing - the circular velocities produced by the baryonic component as seen from an inertial frame of reference (e.g. the blue curve in Fig. 1). Taking this into account and extracting $V_{dark}(r)$ from Eq. (4) gives:

$$V_{dark}(r) = \sqrt{\omega^2 r^2 + 2\omega r V_{baryonic}(r)}, \quad (5)$$

where $V_{dark}(r)$ denotes the circular velocities of bodies orbiting an effective dark halo; that is, a dark halo which produces the same velocity field (and gravitational field) as fictitious forces do. Assuming a spherically symmetrical effective halo, the density distribution can also be calculated. A short derivation gives:

$$\rho_{dark}(r) = \frac{\omega}{4\pi G}(3\omega + 4\frac{V_{baryonic}(r)}{r} + 2V'_{baryonic}(r)). \quad (6)$$

As can be seen in equations 5–6, the effective halo is characterized by some unique features. First, the distribution of baryons is embedded within the effective halo. This coupling between dark and baryonic matter in spiral galaxies has been discussed extensively in the literature (Persic, Salucci & Stel, 1996; Salucci & Burkert, 2000; Swaters et al., 2012; McGaugh, 2014). Here, this connection is a natural characteristic of the effective halo. Second, the effective halo includes a single free parameter (i.e. ω). Most of the common dark-halo profiles include two free parameters (e.g. the virial mass and the concentration parameter). However, these two parameters are known to be observationally correlated (Burkert, 1995; Jimenez, Verde & Oh, 2003). Therefore, in practice, common dark halos as well as effective dark halos can be expressed with a single free-parameter. It is worth mentioning that the mass-to-light parameter (hiding in $V_{baryonic}(r)$) was not counted as an additional parameter since it has to be set also when real dark halos are used.

Next, we plot the effective-halo profile together with common dark-halo profiles. The dependence of the effective halo on $V_{baryonic}(r)$, however, compels us to do so only per given galaxy. In Fig. 3 we use three different galaxies in order to compare between a Burkert dark halo (Burkert, 1995), an NFW dark halo (Navarro, Frenk & White, 1997) and our effective halo. For each galaxy we draw the density distribution and the circular-velocity distribution of each halo. In order to set the free parameters of each halo we use the RCs data of McGaugh (2017). For each galaxy, we choose the halo parameters which produce the best-fit to the data, using a fixed M/L for the baryonic component. The process of fitting the data is explained in section 4. The values and the actual distributions are presented in the figure.

Looking at each panel of Fig. 3, the main result is the similarity between the distributions. In general, it seems that non-inertial effects can reproduce the behavior of dark halos. Considering the density profiles, one can notice that the effective-halo distribution in the inner regions is less steep than that shown by NFW. Thus, the effective halo may not suffer from the difficulties that the NFW profile experience due to its "cuspy" behavior (de Blok, 2010). In the central region, the effective halo mostly follows the NFW behavior, while in the outer regions it has a "tail". Let us note that the effective halo cannot reproduce all the different shapes that NFW or Burkert support. It can imitate their shapes only when their parameters are tuned to fit real data. Specifically, in the cases we present here, the parameters' values are consistent with a "maximal" disk, i.e. the contribution of the dark halos in the inner regions is small.

4 APPLYING THE NEW MODEL ON A SAMPLE OF DISK GALAXIES

In section 2, we suggested that the new model for the rotational velocities should include an additional term (ωr). This additional term arises in non-inertial systems. It represents the additional tangential velocity relative to these systems. In section 3, we demonstrated that such a term can effectively "play the role" of a dark halo. Its contribution to the circular velocities (at least in the examined test cases) is practically similar to the contribution of NFW or Burkert. The next natural step would be to fit a large number of rotation curves using the new model.

When fitting a rotation curve, one should first model the galaxy's mass distribution. This can be done either analytically or numerically. When taking the analytical approach the galaxy is traditionally divided into its main components. Then, the contribution of each component to the circular velocity is calculated separately. Examples of such components may include a Freeman disk (Freeman, 1970), an Hernquist bulge (Hernquist,

Preprints (www.preprints.org) | NOT PEER-REVIEWED | Posted: 28 October 2020 doi:10.20944/preprints202010.0586.v1

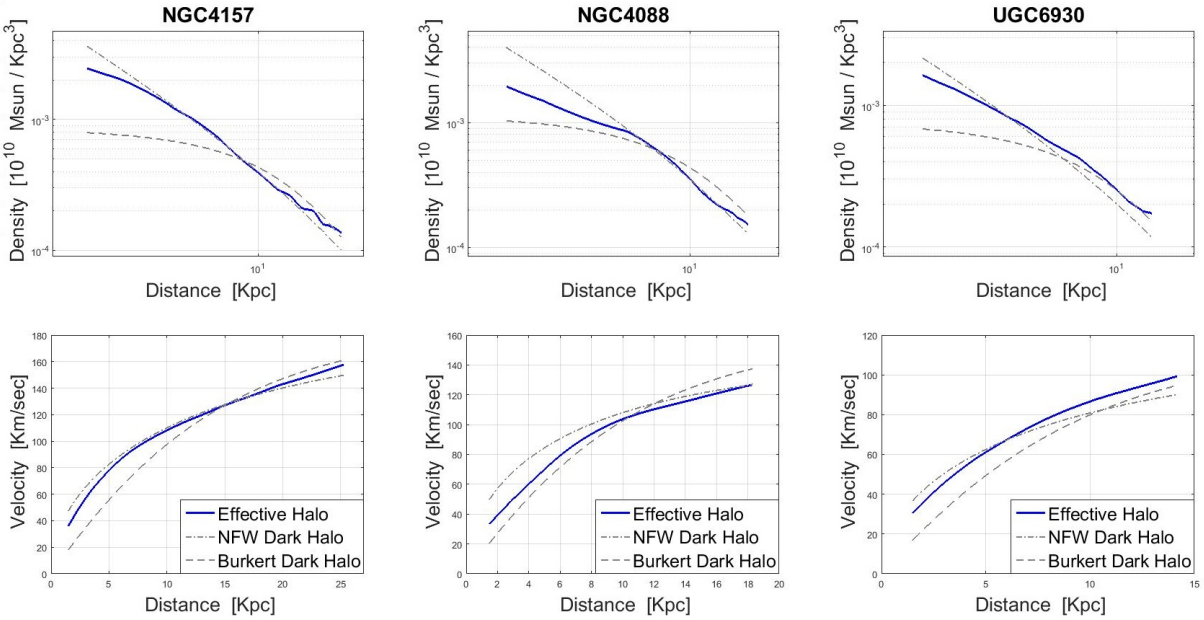

Figure 3. Density distributions of Burkert, NFW, and the effective halo are plotted in the upper panels. The corresponding rotational velocities are given in the lower panels. The Burkert and the NFW halos use two free parameters: The virial mass, Mvir [10^{10} Msun] and the concentration parameter, c. The effective halo has one parameter, namely ω [10^{-16} rad/sec]. Left Panels: NGC 4157 (NFW: Mvir = 170 , c = 5; Burkert: Mvir = 120 , c = 12; effective halo: ω = 1.12). Middle Panels: NGC 4088 (NFW: Mvir = 70 , c = 7; Burkert: Mvir = 70 , c = 13.5; effective halo: ω = 1.04). Right Panels: UGC 6930 (NFW: Mvir = 40 , c = 5; Burkert: Mvir = 30 , c = 11.5; effective halo: ω = 1.17).

1989) and gaseous disk (Toomre, 1963). The derivation of the gravitational field (and circular velocities) of each component assumes the validity of Newton's laws. Therefore, the circular velocities predicted by these models are valid only with respect to inertial frames of reference.

This conclusion also holds when a numerical approach is taken. Modern techniques use the observed light distribution of a galaxy as a tracer for the galaxy's mass distribution. The gravitational field and the circular velocities are then derived numerically. A detailed description of such a process can be found in Sanders & McGaugh (2002). In this section, we follow the same process in order to calculate the inertial velocities for a sample of disk galaxies. Unless a bulge is present, a single parameter is required: the stellar mass-to-light ratio of the disk (M/L), which is assumed to be constant for a given galaxy. The Newtonian (inertial) velocity is then given by:

$$V_{inertial}(r) = V_K(r) = \sqrt{(M/L) \cdot v^2_{disk}(r) + v^2_g(r)}, \quad (7)$$

where M/L is the free parameter, $v_{disk}(r)$ is the numerically-derived stellar-disk contribution and $v_g(r)$ is the numerically-derived gaseous-disk contribution. In this work, the model contributions $v_{disk}(r)$, $v_g(r)$ for each individual galaxy, as well as the observed RCs, were kindly provided by McGaugh and can be found in McGaugh's Data Pages (McGaugh, 2017). The sample of galaxies we use here is based on the sample used by McGaugh in his Baryonic Tully-Fisher work (McGaugh, 2005). It includes galaxies with extended 21-cm rotation curves spanning a large range of luminosities, radii, and flat rotation velocities. For the sake of simplicity, only galaxies without a bulge contribution were selected.

According to the new model, an additional term (ωr) should be added to the inertial velocities in order to predict the observed velocities. The new model, therefore, includes two free parameters: M/L and ω. For each galaxy, we use the least-squares method in order to find the best-fit values for the two parameters; i.e. the values that give the minimum-χ^2. In Fig. 4 we present a fair selection of our fits to RCs. The rest of the fits and a table summarizing the best-fit parameters can be found in Appendix B.

Looking at Fig. 4, the first outcome is the dominance of the Newtonian curve in the inner regions of the RCs. Inside the inner regions, where the linear term is still small, the Newtonian term almost fits the data. In fact, it is similar to the "maximum-disk" approach, where the dark-halo contribution in the inner regions is still small, and the baryonic curve almost fits the

Preprints (www.preprints.org) | NOT PEER-REVIEWED | Posted: 28 October 2020 doi:10.20944/preprints202010.0586.v1

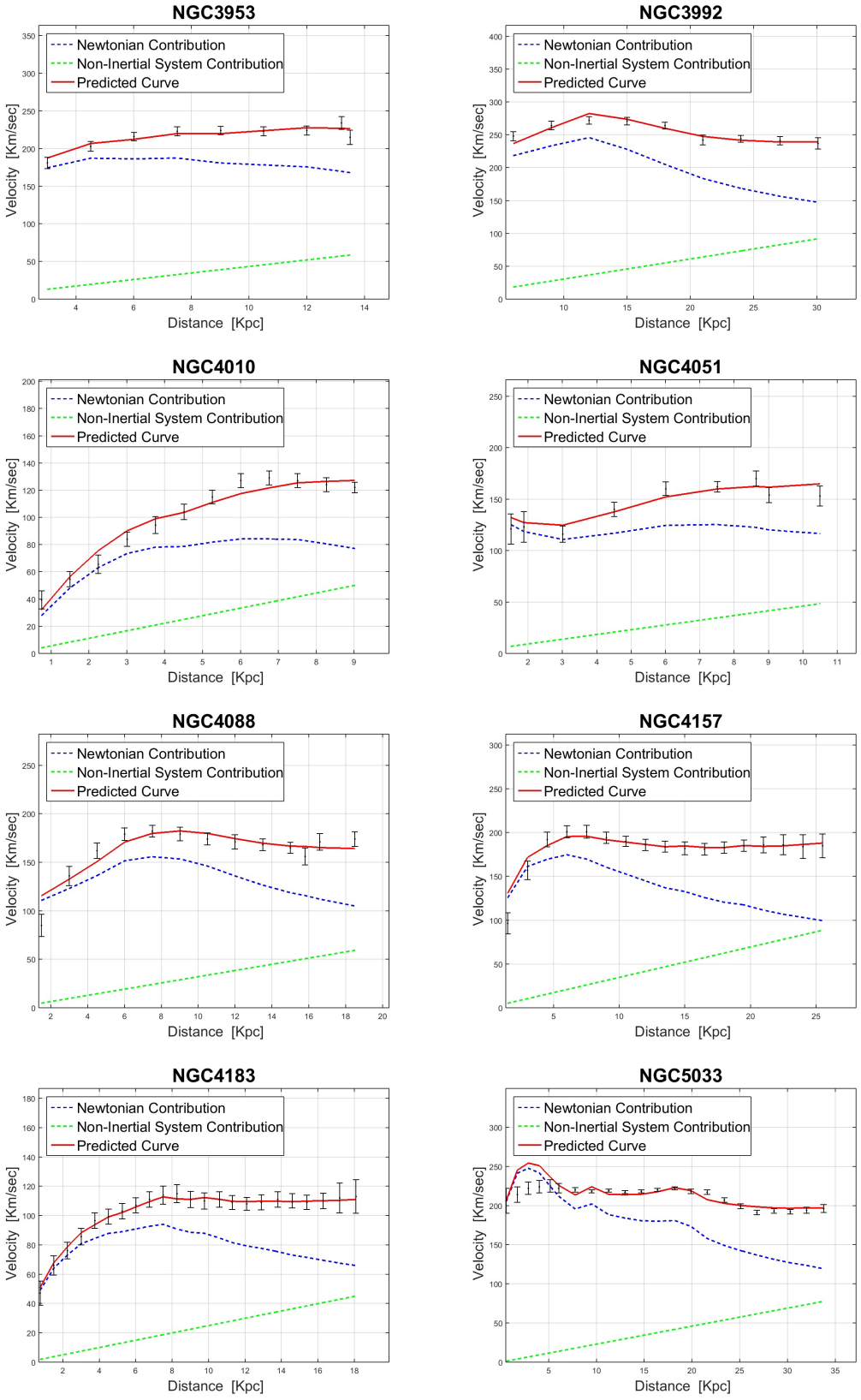

Figure 4. RCs for the different galaxies are presented. In each panel one can see the measured values (black error bars) together with the predicted curve (red line). The dashed blue curve corresponds to the Newtonian term $v_k(r)$ while the dashed green line corresponds to the linear correction term ωr.

Preprints (www.preprints.org) | NOT PEER-REVIEWED | Posted: 28 October 2020 doi:10.20944/preprints202010.0586.v1

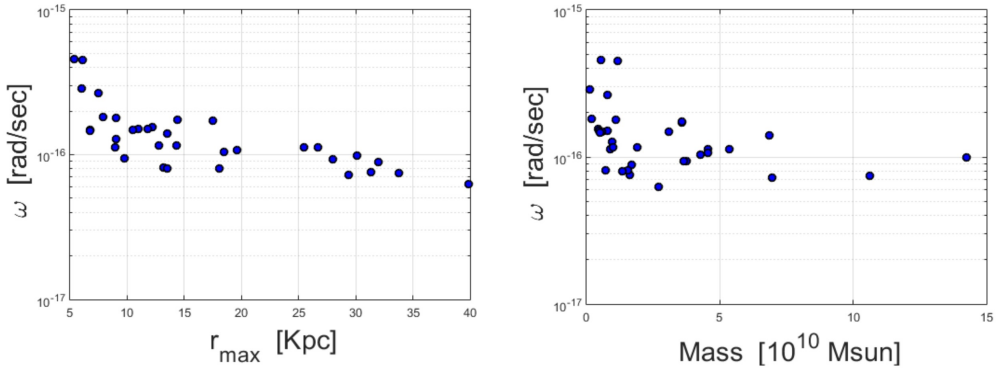

Figure 5. Left panel: a scatter plot of the best-fitted ω's vs r_{max} (the last point of the RC). Right Panel: a scatter plot of ω vs the galaxy's mass. Both plots were produced using the sample of galaxies summarized in Appendix B.

data. This result is very important. When using a dark halo without adopting the maximal-disk approach, a degeneracy between the disk and the halo is usually revealed (Dutton et al., 2005; Geehan et al., 2006). Our model eliminates the degeneracy but still provides very accurate results.

Another natural outcome is the consistency of the fits with Renzo's experimental law (Sancisi, 2004). This law states that every time a feature arises in the radial light distribution, the rotation curve shows a corresponding feature. These features should clearly be evident in the inertial (baryonic) velocities $V_K(r)$, as those were directly derived from the light distributions. In our case, the predicted curves are obtained simply by adding a linear term to the inertial velocities; thus the features are preserved. NGC 1560 (see Appendix B) is a good example: it can clearly be seen that the small "bump" in the data (at 5 Kpc) has a corresponding "bump" in the predicted curve. Common dark halos usually struggle to predict these "bumps" (Gentile et al., 2010).

The next point deals with the M/L values. Looking at Table 2 (given in Appendix B) one can notice that the fitted values are quite reasonable. The median value of the population is 1.5 $[M_{sun}/L_{sun}]$ while the median absolute deviation is 0.5 $[M_{sun}/L_{sun}]$.

The last point deals with the fitted values of our new parameter, ω. First, only positive ω's were obtained in the fits. This means that the local inertial frame K is "dragged" relative to the observational frame K' in the same direction as the direction of the revolving matter in each and every galaxy. This is consistent with our initial expectations since the rotational direction of a galaxy was found to be coherent with the average motion of neighbor galaxies (Lee et al., 2019). If indeed the inertial frame K is rotating relative to the observational frame K', then the cause for such a rotation could well be originated in this average motion of background galaxies. Second, as can be seen in Fig. 5, the values of ω correlate with other galaxy parameters. In the left panel one can see that the larger the radius of a galaxy (represented here by the last point of the RC), the smaller the value of ω. In the right panel one can see a similar trend (although weaker) with the galaxy's total (baryonic) mass. A deeper understanding of these correlations may require the construction of a general-relativistic model which takes into account the effects found by Lee et al. (2019).

5 SUMMARY AND FUTURE DIRECTIONS

Thus far, two main approaches have been taken in order to deal with the discrepancy in galaxy rotation curves: changing the underlying laws of physics, or adding more mass to the detectable mass distribution. The additional inward attraction, in both cases, result in corrected rotational velocities. In the scope of this work, we have shown that the different dynamics in the presence of inertial forces also lead to corrected rotational velocities. In fact, these new rotational velocities strongly resemble those obtained by using dark-halo profiles.

The motivation for proposing that fictitious forces may arise relative to the observational frame of a galaxy originated in two complementary arguments. First, the assumption that the observational frame (K') is inertial was not tested. It was taken as "ground truth" mostly due to its implicit nature. Testing such an assumption may require a model that takes into account the various possible phenomena (in different scales) that affect the determination of a local inertial frame. Second, the unexpected findings of Lee et al. (2019) support a scenario of non-inertial K'. As was discussed in Section 2, the rotation of background matter can, in general, produce fictitious forces in K'. However, modeling or

Preprints (www.preprints.org) | NOT PEER-REVIEWED | Posted: 28 October 2020 doi:10.20944/preprints202010.0586.v1

explaining these observations is not included in the scope of this work.

Here, we have demonstrated that a single degree of freedom is sufficient in order to represent the possible relative motion between the observational frame (K') and the local inertial frame (K) of a given disk galaxy. Relying on this degree of freedom, we have shown that the additional gravitational field in K' due to fictitious forces resembles the gravitational field of a dark halo. Additionally, we developed a model that predicts the (non-inertial) rotational velocities in K'. Applying the new model to a wide sample of RCs produced very accurate results.

The idea that the observed velocities might be non-inertial can be generalized, in principle, to other types of galaxies. However, the specific model we developed here is applicable only to disk galaxies. It might be interesting, therefore, to search for equivalent models in the field of elliptical galaxies; that is, to explore the discrepancy in measured velocity dispersions. Another interesting direction for further investigation is to model galactic formation in the presence of inertial forces. If those would indeed turn out to be relevant in rotation curves, then their role in galaxy formation might be important as well.

The discrepancy in galaxy rotation curves is probably one of the most surprising discrepancies in astrophysics. It seems to puzzle us even today, decades after it was first discovered.

6 ACKNOWLEDGEMENTS

We wish to thank Stacy McGaugh for sharing his data and for valuable advice. In addition, we would like to thank Meir Zeilig-Hess and Oran Ayalon for helpful insights.

DATA AVAILABILITY

The data underlying this article are available in DATA SECTION, at http://astroweb.case.edu/ssm/data. It includes extended 21-cm rotation curves as well as B-band photometry for the sample of galaxies analyzed in this work.

A DEFINING THE OBSERVATIONAL FRAME

The goal of this appendix is to remind the reader how the rotational velocities of a galaxy are derived (i.e. the data points in an RC), and to provide a well-defined system of coordinates relative to which these rotational velocities are given.

In general, the process of deriving a rotation curve could be separated into two steps: first, measure the *line-of-sight velocities* in a galaxy (i.e. the 2D velocity field); second, convert these line-of-sight velocities into rotational velocities (Swaters et al., 2009). Before proceeding, a crucial clarification is needed: the line-of-sight velocity of an object is a component of the object's total velocity along the line of sight. The object's total velocity, by definition, must be given relative to some frame of reference. Therefore, if an object's total velocity is to be calculated from the line-of-sight velocity (e.g. by some geometrical considerations), then it is necessary to provide the corresponding frame as well.

The most basic conversion between line-of-sight velocities and circular velocities uses only the line-of-sight velocities located on the main axis of the galaxy's projected image, and assumes a single fixed value for the disk inclination (de Blok et al., 2008). In this case, the conversion is simply given by:

$$v_c(r) = \frac{v(r) - v_{sys}}{sin(i)}, \tag{8}$$

where $v_c(r)$ are the rotational velocities (e.g. the black data points in Fig. 1), $v(r)$ are the line-of-sight velocities, v_{sys} is the galaxy's systemic velocity, and i is the inclination angle of the galactic plane ($i = 90^o$ for edge-on galaxies). Relying on this simple transformation would not change the conclusions we draw at the end of this section.

As noted before, the reference frame (relative to which the rotational velocities $v_c(r)$ are given) is in fact determined when using such a relation. Actually, it is not fully determined, but strongly constrained. It turns out that any reference frame in which the systemic velocity of a galaxy vanishes and the line-of-sight is stationary (i.e. does not rotate), can be regarded as valid. To illustrate this, let us focus on the (unrealistic) example in which $v_{sys} = 0$, $sin(i) = 1$. In this case, relation 8 states that the rotational velocities are equal to the measured line-of-sight velocities. However, as can be seen in Fig. 6, this statement holds only relative to system K', where the line of sight is stationary. In any reference frame which is rotating relative to K', the rotational velocity would take a different value, the line of sight wouldn't be fixed and relation 8 wouldn't hold. The reader may take a minute to be fully convinced at this point.

Now, let us define one specific reference frame which satisfies the above requirement (i.e. a frame, relative to which the rotational velocities are given). We define a frame whose fundamental plane coincides with the galaxy plane and its origin coincides with the galactic

 doi:10.20944/preprints202010.0586.v1

Galaxy	ω^a	M/L^b	Galaxy	ω	M/L
M33	1.12	0.97	NGC 4085	4.58	0.50
NGC 5033	0.74	5.06	NGC 4088	1.04	1.16
NGC 1560	1.82	2.57	NGC 4100	1.07	2.36
NGC 247	1.51	1.76	NGC 4157	1.12	2.27
NGC 300	1.55	0.96	NGC 4183	0.81	1.45
NGC 3726	0.93	1.19	NGC 4217	1.73	1.72
NGC 3877	0.94	1.78	NGC 5585	1.50	0.87
NGC 3893	1.71	1.43	NGC 6946	0.72	0.79
NGC 3917	1.16	1.58	NGC 7793	1.49	1.40
NGC 3949	4.51	0.48	UGC 128	0.63	3.49
NGC 3953	1.40	2.25	UGC 6446	0.81	1.70
NGC 3972	2.66	1.00	UGC 6667	1.47	1.74
NGC 3992	0.99	4.26	UGC 6818	2.86	0.16
NGC 4010	1.80	1.37	UGC 6917	1.28	2.01
NGC 4013	1.13	2.90	UGC 6930	1.17	1.30
NGC 4051	1.49	1.11	UGC 6983	0.80	3.11

Table 1 Best-fitted parameters of each galaxy.

[a] ω is given in $[10^{-16} rad/sec]$.
[b] M/Ls are given in the B-band, in units of $[M_{sun}/L_{sun}]$.

center. We also set the frame in such a way that the line-of-sight of the observer is stationary (in the simple case of an edge-on galaxy, the primary axis is pointing towards the observer). This frame of reference is denoted in the main text as K'. It turns out that frame K' might be non-inertial (see section 2).

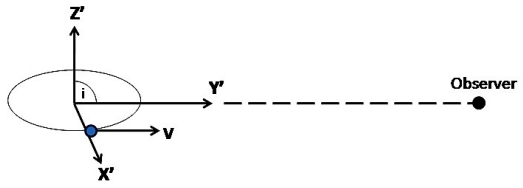

Figure 6. A stationary distant observer is located on the $y'-axis$ (i.e. $v_{sys}=0$, $sin(i)=1$). Such an observer would measure a value of V for the line of sight velocity, thus, relying on relation 8, would extract a value of V for the rotational velocity. As can be seen in the figure, this value is valid relative to the system K'. At any other frame which is rotating relative to K', the rotational velocity would take a different value.

B RC FITTINGS

The RC fittings for the entire sample as well as the best-fitted parameters of each galaxy are given in the next pages.

REFERENCES

Babcock H. W., 1939, Lick Observatory Bulletin 19, 41
Brill D. R., Cohen J. M., 1966, Physical Reviews 143
Burkert A., 1995, ApJ, 447, L25
Carignan C., 1985, ApJ, 299, 59
Corbelli E., Salucci P., 2000, MNRAS, 311.2, 441
de Blok W.J.G., 2010, Advances in Astronomy , 2010
de Blok W.J.G. et al., 2008, AJ, 136, 6
del Popolo A., 2007, Astron.Rep, 51, 169
Dutton A. et al., 2005, ApJ, 619, 1
Einstein A., 1920, Relativity: The special and general theory, Penguin, 4
Freeman K.C., 1970, ApJ, 160
Geehan J. J.,Fardal M. A. ,Babul A. , Guhathakurta P., 2006, MNRAS, 366.3, 996
Gentile G. et al., 2010, MNRAS, 406, 4
Hernquist L., 1989, ApJ, 356, 359
Jarosik N. et al., 2011, ApJS, 192, 14
Jimenez R., Verde L., Oh S.P., 2003, MNRAS, 339, 243
Lee J.H. et al., 2019, ApJ, 884, 2
Markevitch M. et al., 2004, ApJ, 606, 2
Massey R., Kitching T., Richard J., 2010, Reports on Progress in Physics , 73
McGaugh S., 2017, McGaugh's Data Pages. N.p., n.d. Web. 22 Jan. 2017, <http://astroweb.case.edu/ssm/data/>
McGaugh S., 2014, Galaxies , 2, 601
McGaugh S., 2005, ApJ, 632, 859
Milgrom M., 1983, ApJ,270, 365
Navarro J., Frenk C., White S., 1997, ApJ, 490, 493
Persic M., Salucci P., Stel F., 1996, MNRAS, 281, 27
Rubin V. C., Ford W. K. Jr, Thonnard N., 1980, ApJ, 238, 471
Salpeter, E., 1978, Symposium - International Astronomical Union, 77, 23
Salucci P., Burkert A., 2000, ApJ,537, L9
Sancisi R., 2004, IAU Symposium, Vol 220
Sancisi R., van Albada T.S., 1987, Symposium - International Astronomical Union, 117, 67-81.
Sanders R., McGaugh S., 2002,ARA&A, 40, 217
Schmid C., 2006, Physical Review D, 74
Sofue Y., Rubin V. C., 2000,ARA&A, 39, 137
Swaters R., Sancisi R., van Albada T.S., van der Hulst J.M., 2009, A&A , 493, 871
Swaters R., Sancisi R., van der Hulst J.M., van Albada T.S., 2012, MNRAS, 425.3, 2299
Thirring, H., 1918, physicalische zeitschrift , 19, 33
Toomre, A., 1963, ApJ, 138, 385

Preprints (www.preprints.org) | NOT PEER-REVIEWED | Posted: 28 October 2020 doi:10.20944/preprints202010.0586.v1

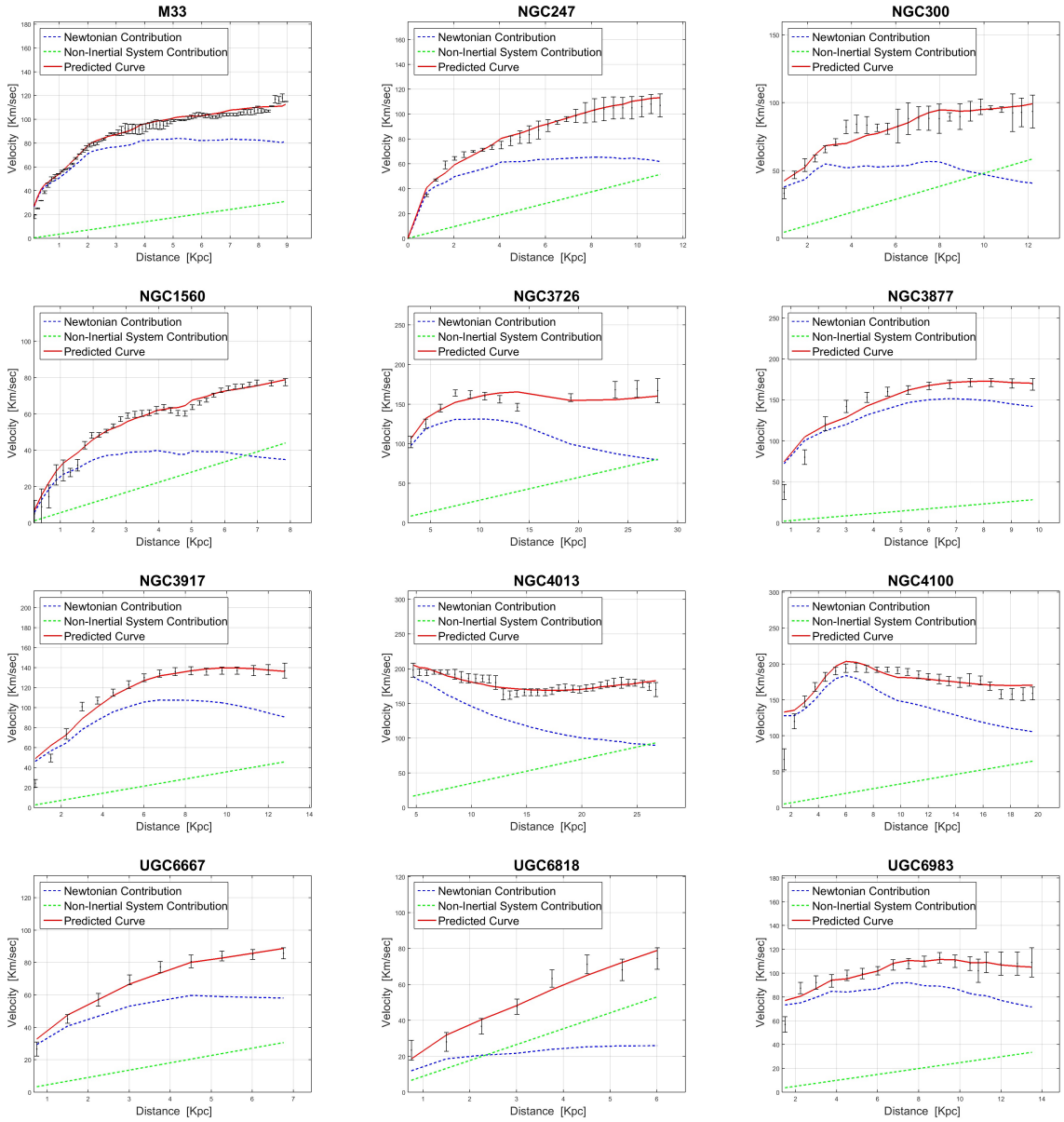

Preprints (www.preprints.org) | NOT PEER-REVIEWED | Posted: 28 October 2020 doi:10.20944/preprints202010.0586.v1

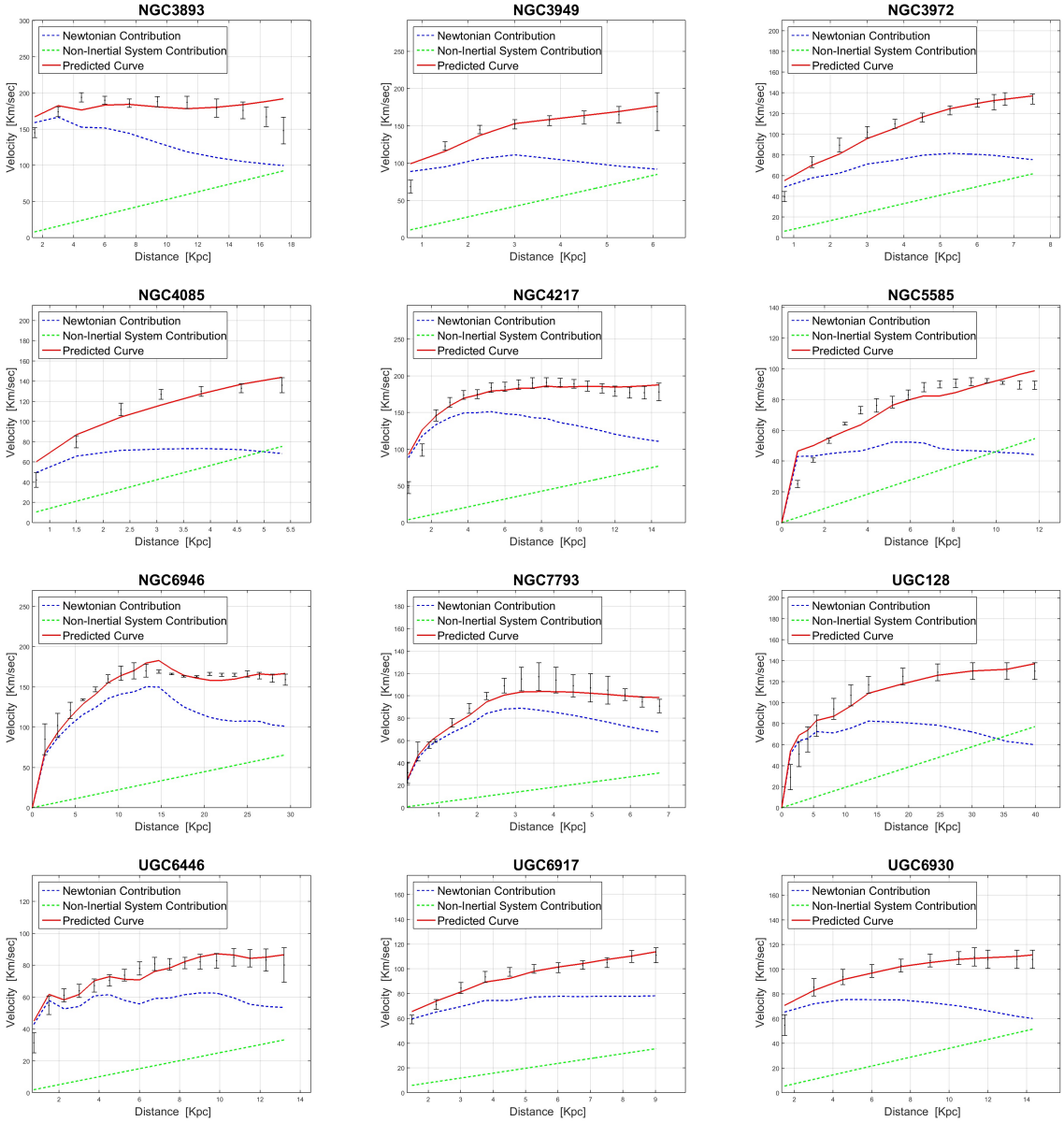

Figure 7. RCs for the different galaxies are presented. In each panel one can see the measured values (black error bars) together with the predicted curve (red line). The dashed blue curve corresponds to the Newtonian term $v_k(r)$ while the dashed green line corresponds to the linear correction term ωr.